Simultaneous collision-induced transitions in H2O+CO2 gas mixtures

H Fleurbaey, Didier Mondelain, W Fakhardji, J M Hartmann, A Campargue

Simultaneous collision-induced transitions in H_2O+CO_2 gas mixtures

H. Fleurbaey[a], D. Mondelain[a], W. Fakhardji[b], J.-M. Hartmann[b], A. Campargue[a*]

[a] *Univ. Grenoble Alpes, CNRS, LIPhy, 38000 Grenoble, France*
[b] *Laboratoire de Météorologie Dynamique/IPSL, CNRS, Ecole Polytechnique, Institut polytechnique de Paris, Sorbonne Université, Ecole Normale Supérieure, PSL Research University, F-91120 Palaiseau, France*

Key words

Absorption spectroscopy; Radiative transfer; Collision Induced Absorption; Continuum

[*] Corresponding author: alain.campargue@univ-grenoble-alpes.fr; LIPhy, Bat. E, 140 rue de la Physique, 38400 Saint-Martin d'Hères (France).

Abstract

A collision induced absorption (CIA) band has been measured near 6000 cm^{-1} in a spectrum of humidified CO_2 recorded by cavity ring down spectroscopy (CRDS) at low pressure (<1 atm). This absorption adds a contribution to the H_2O+CO_2 continuum mostly originating from far wings of the CO_2 and H_2O resonance lines broadened by collisions with H_2O and with CO_2, respectively. The observed CIA corresponds to a simultaneous excitation of $^{12}CO_2$ and H_2O colliding molecules in the ν_3 antisymmetric and ν_1 symmetric stretching mode, respectively. CRDS spectra recorded near 5940 cm^{-1} with a highly enriched $^{13}CO_2$ sample provide a confirmation of the assignment since the measured CIA isotopic spectral shift (of about -68 cm^{-1}) coincides with that between the ν_3 bands of $^{12}CO_2$ and $^{13}CO_2$. The integrated binary coefficient of the two CIA is evaluated and found to be on the order of 2.3×10^{-3} $cm^{-2}amagat^{-2}$. Classical molecular dynamics simulations (CMDS) of the considered CIA are also presented, based on the dominant dipole induction mechanism associated with the vibrational matrix elements of the dipole of CO_2 (ν_3) and isotropic polarizability of H_2O (ν_1). The results of the calculations are found in good agreement with the observations, thus further validating the attribution of the observed CIA structure to the above mentioned double transitions.

I. Introduction

The absorption of light by pure water vapor involves two contributions. The first one is the monomolecular absorption due to the rovibrational resonance lines which is proportional to the water vapor pressure. The second one, varying smoothly with the frequency, is the so-called water vapor self-continuum, which is proportional to the squared molecular density as it is due to interactions between pairs of water molecules. Various processes may contribute to this continuum, which include the far wings of the resonance lines, collision-induced absorption (CIA), and dimers. Similarly, the absorption spectrum of pure carbon dioxide involves resonance lines and a self-continuum contribution again resulting from the three processes mentioned above generating absorptions proportional to the squared gas density. Numerous experimental and theoretical studies have been devoted to the self-continua of both H_2O and CO_2 (see [1] and chapters V and VI of [2]) due to their importance for radiative transfer processes in the atmospheres of the Earth and Venus, respectively.

However, the self-continua are not the only continua relevant for planetary applications. Since planetary atmospheres are mixtures of various molecular species, there are additional "crossed" absorption contributions, proportional to the product of the densities of the different colliding molecules. This is obviously the case for the Earth atmosphere in which the H_2O- and CO_2-air (or N_2) continua play, together with the H_2O self-continuum, a significant role which has motivated a large number of studies (see [1] and chapters V and VI of [2]). Note that, until recently, it was generally considered that the associated atmospheric continua were essentially due to the far wings of the air-broadened lines of H_2O and CO_2. The limits of this assumption were pointed out a few years ago with the demonstration of the importance of an N_2 absorption band induced by collisions with H_2O in the H_2O-N_2 continuum [3,4]. Due to its potential importance for the atmospheres of Early Mars and exoplanets, the continuum in H_2O-CO_2 mixtures has recently received a renewed attention, nearly 30 years after pioneer studies devoted to the CO_2-broadened line wings of H_2O for Venusian studies [5,6]. Measurements and calculations have been made in order to characterize the influence of collisions with H_2O on the wings of CO_2 lines [7,8,3] as well as that of collisions with CO_2 on the wings of H_2O lines [7,9].

Very recently, we have undertaken a series of measurements aiming to characterize the absorption continuum of H_2O-CO_2 mixtures in the 1.6 µm and 2.3 µm windows and near 3.5 µm, corresponding to low opacity regions for both CO_2 and water vapor [10]. The "crossed" absorption (proportional to the product of the H_2O and CO_2 densities) was observed to include an unexpected broad band, centered near 6000 cm^{-1}, in addition to the contributions of the far wings of the lines of the monomers (note that pure CO_2 spectra do not exhibit any CIA band in this spectral region [11]). On the basis of the spectral position of its center, this band was tentatively assigned to the simultaneous collision-induced transitions involving a ν_1 (Raman) excitation of H_2O and a ν_3 (dipole absorption)

excitation of $^{12}CO_2$ [noted $\nu_3(CO_2)+\nu_1(H_2O)$, hereafter] but no further analysis was made. Note that such simultaneous transitions (sometimes also denoted as double transitions), resulting from the polarization of one molecule (*e.g.* through a vibrational matrix element of the polarizability) by the vibrating electric field of the collision partner (*e.g.* through a vibrational matrix element of the electric dipole or quadrupole) have been observed and analyzed for diverse molecular systems involving H_2 or N_2 (e.g. [12,13,14,15]), but also for pure CO_2 [16] and CO_2-N_2 [17,18,19,20,21].

In this paper, we revisit the $\nu_3(CO_2)+\nu_1(H_2O)$ CIA band both experimentally, by complementing the natural CO_2 measurements reported in Ref. [10] by a new investigation using $^{13}CO_2$, and theoretically, by using a simple induction model and molecular dynamics simulations. In the next section, we summarize the conditions of the acquisition of the humidified CO_2 spectra by cavity ring down spectroscopy (CRDS). The different steps of the CIA retrieval by successive subtraction of the different contributions from the measured spectra are also described in this section. In section 3, the classical molecular dynamics simulations (CMDS) and the input data used for the prediction of the CIA are described. The measured and calculated results are then presented and discussed in Sec. 4, before concluding remarks (Sec. 5).

2. CRDS recordings and CIA retrieval

2.1. Data acquisition

The inherent sensitivity and baseline stability of cavity enhanced techniques make them particularly suitable to measure weak continua [22]. They, in particular, enable to use samples at sub-atmospheric pressure while traditional methods are generally combined with pressurized cells. This is crucial in the case of mixtures involving water vapor at room temperature, the limitation by the saturation pressure making accurate absorption measurements by FTS with long absorption pathlengths practically impossible in the atmospheric transparency windows. In contrast, measurements by CRDS and OFCEAS have recently led to accurate determinations of the self- and foreign (air)-continua of H_2O [23,24,25,26,27,28]. Another advantage of recordings at sub-atm pressures is that the contribution of local absorption transitions is easier to calculate and remove, since line-mixing effects may be disregarded and isolated line shapes can be used. For instance, CRDS was recently applied to the characterization of the O_2 CIA band at 1.27 µm both at NIST [29] and in our laboratory [30,31]. The use of low O_2 pressures enabled to minimize the impact of line mixing effects on the CIA determination obtained with an agreement of less than 1% between the two datasets at room temperature.

The $\nu_3(CO_2)+\nu_1(H_2O)$ CIA band was observed in CRDS spectra of humidified CO_2 recorded in the 5725-6665 cm^{-1} and 5856-5986 cm^{-1} intervals, for natural CO_2 and $^{13}CO_2$ samples, respectively. Distributed feedback (DFB) laser diodes were used as light sources, each of them covering a spectral

range 20 to 30 cm^{-1} wide by temperature variation. The cavity-ring down spectrometer used a 142 cm long high finesse cavity fitted with two highly reflective dielectric mirrors. Ring down (RD) times were of the order of 120 to 160 µs. Typically, ten RD times were averaged at each spectral step separated by 0.005 cm^{-1}. A part of the laser light was sent into a wavelength meter (model 621-A IR from Bristol) to monitor the laser frequency.

As detailed in Ref. [10], the spectra with natural CO_2 were recorded in flow regime using H_2O+CO_2 mixtures with H_2O molar fractions between 3000 and 15000 ppmv. The gas flow of the mixture (typically a few tens sccm inside the CRDS cavity) was produced using a commercial humidity generator (from Omicron Technologies). The total pressure in the CRDS cavity was monitored by a sensor from Edwards (1000 mbar full scale, accuracy 0.15 % of reading) and maintained at a fixed value of 400 or 750 Torr with a solenoid valve and a software-based proportional integral loop acting on the gas flow. The densities of CO_2 and H_2O (ρ_{CO2} and ρ_{H2O}, respectively) were obtained from the partial pressures and the cell temperature measured with a calibrated Pt100 sensor (2σ-uncertainty ±0.06°C) fixed on the external wall of the cavity underneath the enveloping thermal insulation foam.

In the case of the recordings with humidified $^{13}CO_2$, the limitation of the gas consumption (imposed by the cost of the ^{13}C enriched CO_2 tank) required to record the spectra in static regime. The cell was thus first filled with about 6.5 Torr of water vapor and $^{13}CO_2$ (from Aldrich, 99 % ^{13}C enrichment) was then added up to a total pressure of 400 Torr.

The baseline determination of the spectra relied on measurements performed with argon before and after the recording with the (H_2O+CO_2) mixture, with the cavity pumped before each gas filling (argon or mixture). The two argon spectra ensure that the cavity alignment (and thus the baseline) is unchanged after pumping/filling cycles. By comparing the two argon spectra, the baseline stability was found to be of the order of a few 10^{-10} cm^{-1}. In order to check the proportionality of the retrieved "crossed" absorption to the $\rho_{CO2}\rho_{H2O}$ densities product, measurements were performed for several values of the water molar fraction in natural CO_2. The study with $^{13}CO_2$ being mostly performed for validation of the assignment of the observed CIA structure, a single set of experimental conditions (~6.5 Torr of water vapor in $^{13}CO_2$ at a total pressure of 400 Torr) was retained.

2.2. CIA retrieval

After baseline correction, the absorption coefficient, $\alpha(\nu)$, can be expressed as:

$$\alpha(\nu) = M_{CO_2}\rho_{CO_2} + M_{H_2O}\rho_{H_2O} + B_{CO_2}\rho_{CO_2}^2 + B_{H_2O}\rho_{H_2O}^2 + B_{crossed}\rho_{CO_2}\rho_{H_2O} \quad (1)$$

where $M_{CO_2}\rho_{CO_2}$ and $M_{H_2O}\rho_{H_2O}$ are the contributions due to the monomer local lines of CO_2 and H_2O (calculated within a ±25 cm^{-1} range around the center wavenumber), respectively, and ρ represents the density (in $amagat^{-1}$). The B_{H_2O} and B_{CO_2} coefficients (in $cm^{-1}amagat^{-2}$) correspond to the self-continuum coefficients of water and CO_2, respectively. $B_{crossed}$ is the crossed binary coefficient arising

from the interaction of water and CO_2 molecules, thus involving both far line wings (of CO_2-broadened H_2O transitions as well as of H_2O-broadened CO_2 transitions) and CIA bands contributions.

In the case of natural CO_2, the HITRAN2016 database [32] was used to simulate the local CO_2 and H_2O monomer contributions with Voigt profiles truncated at ±25 cm^{-1} excluding the pedestal of the absorption lines (see details in Ref. [10]). The water self-continuum cross-sections B_{H_2O} were taken from Ref. [27] while, for CO_2, the self-continuum cross-sections B_{CO_2} were taken from Ref. [11] or measured in Ref. [10] below and above 5800 cm^{-1}, respectively. The $B_{crossed}$ binary coefficients measured with the natural CO_2 sample for various water vapor molar fractions (from 3000 to 15000 ppm) and two total pressures (400 and 750 Torr) are presented in **Fig. 1**. While over the various experimental conditions the $\rho_{CO_2}\rho_{H_2O}$ density product varied by a factor of 5, the set of retrieved $B_{crossed}$ values are found consistent within about 20 % in the CIA region near 6000 cm^{-1}. **Fig. 1** also includes a fit of the observed band, assuming a Lorentzian shape and fixing the far wing continuum background to its value calculated by the χ-factor approach (see [10]). The parameters obtained from this Lorentzian fit will be discussed in Sec. 4.

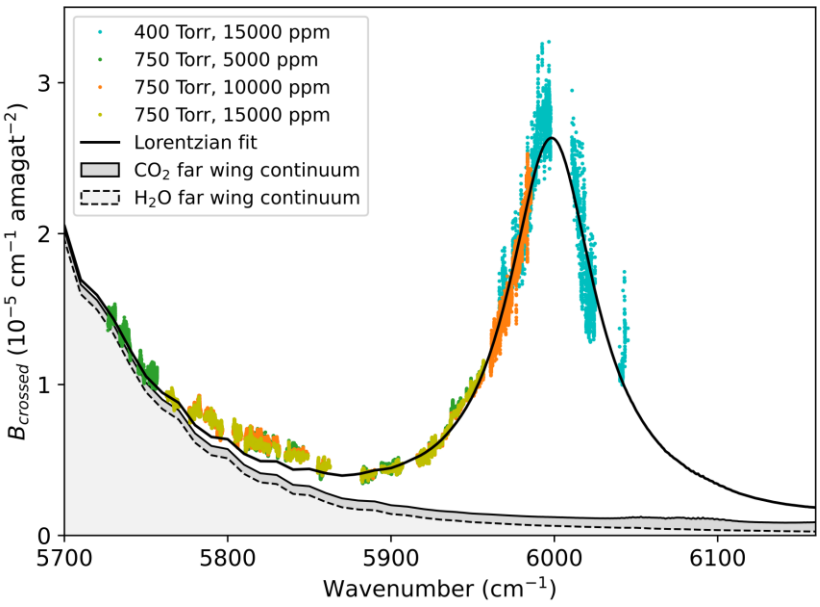

Fig.1: *Overview of the binary coefficients measured in the 5725-6665 cm^{-1} region including the $\nu_3(^{12}CO_2)+\nu_1(H_2O)$ CIA band near 6000 cm^{-1}, for various total pressures and water vapor molar fractions. The best fit of the CIA using a Lorentzian function (black solid line) is superimposed to the far wing continuum background which was fixed to its value calculated by the χ-factor approach (see [10]).*

In the case of humidified $^{13}CO_2$, the measurement of the CIA band is made more difficult because it falls in a region where CO_2 resonance lines are much stronger than with the natural sample. In order to subtract the $^{13}CO_2$ contribution – $(M_{CO_2}\rho_{CO_2} + B_{CO_2}\rho_{CO_2}^2)$ in Eq. (1) – we did not try to simulate separate contributions of the resonance lines and of the self-continuum of $^{13}CO_2$ and preferred to directly subtract a spectrum of dry $^{13}CO_2$ recorded at the same partial pressure of $^{13}CO_2$ as in the

humidified mixture used for the recordings (395 Torr). This, which disregards the effects of collisions with H_2O on the central and wing regions of the $^{13}CO_2$ lines, is of likely small consequences considering the relatively small (1.5 %) amount of water vapor in the humidified sample. **Fig. 2** shows the different contributions to the total absorption coefficient measured for a mixture of about 6 Torr of water in $^{13}CO_2$ at a total pressure of 400 Torr. As adsorption on the walls of the CRDS affected the amount of water in the cell, for the spectral interval corresponding to the tuning range of each DFB laser diode, the water vapor partial pressure, p_{H_2O}, was determined from the integrated absorption coefficient of a few observed water lines. The obtained p_{H_2O} values were found to vary from 5.3 to 7.0 Torr for the six DFB intervals covering the CIA region (5856-5986 cm^{-1}). These p_{H_2O} values were used to calculate and subtract the water self-continuum [27] and the water resonance lines contribution (computed using the HITRAN2016 line list [32]). As illustrated by **Fig. 2**, in our experimental conditions, the two water vapor contributions are much smaller than the $^{13}CO_2$ contribution. After subtraction of the different contributions, the remaining absorption coefficient - $B_{crossed}\rho_{CO_2}\rho_{H_2O}$ - shows a clear bell shape centered at about 5940 cm^{-1} corresponding to the $\nu_3(^{13}CO_2)+\nu_1(H_2O)$ CIA band. Using the determined p_{H_2O} values, the corresponding crossed binary coefficients, $B_{crossed}$, displayed in **Fig. 3** were derived. The obtained curve shows high frequency "noise" due to the imperfect removal of the strong $^{13}CO_2$ resonance lines. An improved description of the CIA band shape is obtained from a Lorentzian fit with a baseline (corresponding to the far wing continuum contribution) assumed to be constant with frequency. The parameters obtained from this fit will be discussed in Sec. 4.

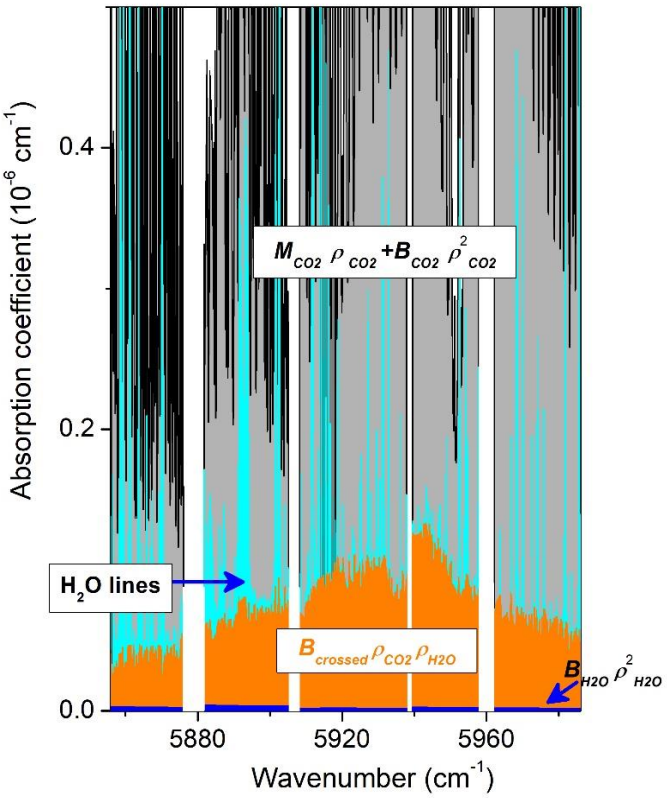

***Fig. 2**: Different contributions to the total absorption coefficient measured by CRDS with a mixture of water and CO_2 highly enriched in ^{13}C. The total pressure was 402 Torr while the water vapor partial pressure varied between 5.3 and 7.0 Torr over the displayed region. The measured absorption coefficient is first reduced by the $^{13}CO_2$ contribution (lines and self-continuum - grey background) measured with a pure $^{13}CO_2$ sample. Then, the water contribution (lines and self-continuum - cyan and blue background, respectively) is simulated and subtracted. The absorption remaining after these subtractions (orange background) shows the bell shape profile of the $v_3(^{13}CO_2)+v_1(H_2O)$ CIA band centered near 5930 cm^{-1}.*

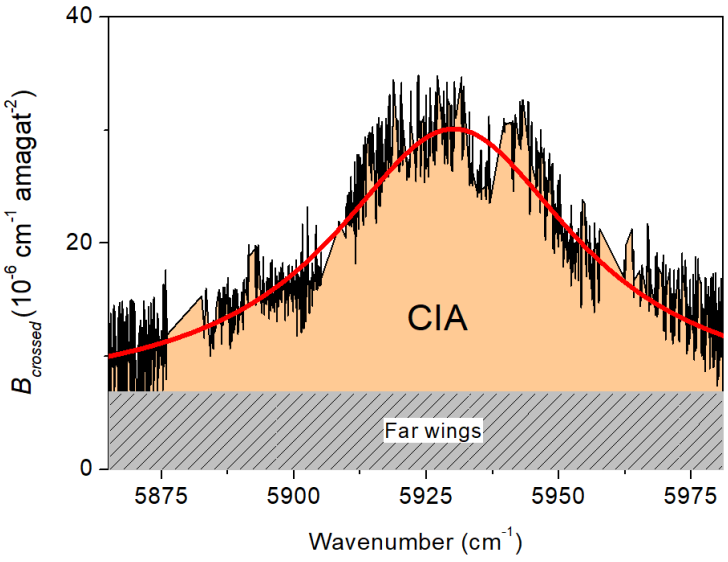

***Fig 3:** Crossed binary coefficients in the region of the $v_3(^{13}CO_2)+v_1(H_2O)$ CIA band. The best fit of the CIA Lorentzian shape (red solid line) is superimposed to the continuum background due to the far wing continuum (dashed). The background level was adjusted by the fit.*

3. Classical molecular dynamics simulations (CMDS)

The CIA in the region of the $\nu_3(CO_2)+\nu_1(H_2O)$ simultaneous transitions was calculated using classical molecular dynamics simulations (CMDS), exactly as described in Ref. [3], with the only difference that the H_2O static isotropic polarizability matrix element $\langle v=0|\alpha_{iso}(\mathrm{H_2O})|v=0\rangle$ used in this previous study was here replaced by the vibrational matrix element $\langle v=0|\alpha_{iso}(\mathrm{H_2O})|v_1=1\rangle$ (here, $v=0$ and $v_1=1$ stand for the (000) and (100) vibrational states of H_2O, respectively). As in Ref. [3], only the component of the induced dipole due to the polarization of H_2O (through its isotropic polarizability $\langle v=0|\alpha_{iso}(\mathrm{H_2O})|v_1=1\rangle$) in the electric field of the CO_2 dipole (through $\langle v=0|\mu(\mathrm{CO_2})|v_3=1\rangle$, where $v=0$ and $v_3=1$ stands for the $(v_1v_2{}^{l_2}v_3)=(00^00)$ and (00^01) vibrational states of CO_2, respectively) was thus taken into account. This is convenient since the induced dipole then does not depend of the orientation of the H_2O molecule but it disregards other induction mechanisms, including the term originating from the anisotropic polarizability of the water molecule (*i.e.* $\langle v=0|\Delta\alpha(\mathrm{H_2O})|v_1=1\rangle$). However note that, as discussed below, this contribution is likely relatively small, while many other terms, such as those involving the product of the H_2O dipole element $\langle v=0|\mu(\mathrm{H_2O})|v_1=1\rangle$ and of the CO_2 polarizability $\langle v=0|\Delta\alpha(\mathrm{CO_2})$ or $\alpha_{iso}(\mathrm{CO_2})|v_3=1\rangle$, vanish due to symmetry considerations. As in Ref. [3], we used $\langle v=0|\mu(\mathrm{CO_2})|v_3=1\rangle=0.13$ a.u. [33, 34]. For H_2O, $\langle v=0|\alpha_{iso}(\mathrm{H_2O})|v_1=1\rangle=0.73$ a.u. was obtained, using the convention of Ref. [35], from the value of α_0^0 provided in Ref. [36] with $\alpha_{iso}=-\alpha_0^0/\sqrt{3}$. Note that our classical calculations lead to a CIA structure that is automatically centered at the sum of the origins of the $\nu_3(^{12}CO_2)$ and $\nu_1(H_2O)$ bands, 2349+3657= 6006 cm^{-1} for $^{12}CO_2$, because all the *Q* transitions of the H_2O ν_1 band, associated with the isotropic polarizability, then have the same imposed wavenumber of 3657 cm^{-1}. This does not correspond to reality since the $(v=0,\ J,K_a,K_c)\rightarrow(v_1=1,\ J,K_a,K_c)$ rovibrational transitions are all shifted to the red with respect to the band origin of 3657 cm^{-1} and spread over typically 10 cm^{-1} [32]. In order to correct for this, the bar spectrum of the true *Q* lines was convoluted by the raw CMDS-predicted CIA, which red-shifts the peak wavenumber by about -6 cm^{-1} with respect to 6006 cm^{-1}. In the case of $^{13}CO_2$, CMDS were computed as done for $^{12}CO_2$, using the same value of $\langle v=0|\mu(\mathrm{CO_2})|v_3=1\rangle$ [37,38], but a change of the ν_3 band origin from 2349 to 2283 cm^{-1}.

4. Results and discussion

As said above, the $^{12}CO_2$ and $^{13}CO_2$ CIA bands as obtained from experiments were fitted assuming a Lorentzian band shape (see **Figs. 1** and **3**). In the case of the main isotopologue, the underlying far wing continuum was fixed to its value calculated by the χ-factor approach (see [10]). In the case of $^{13}CO_2$, the baseline was assumed to be constant with frequency and it was adjusted by the fit. The CMDS-computed spectra for $^{12}CO_2$ and $^{13}CO_2$ were fitted by a Gaussian function to determine the center position, their integration over wavenumber yielded the intensities, and the widths were

determined directly from the computed absorptions. The experimental and calculated centers, integrated areas and half-widths at half-maximum (HWHM) are listed in **Table 1**, calling for several remarks. The first is that the peak positions obtained for measured and computed spectra agree very well. The measured and calculated differences between the $^{12}CO_2$ and $^{13}CO_2$ values, of about 68 cm^{-1}, are in close agreement with the isotopic shift of the $v_3 = 1$ vibrational levels of the two isotopologues (66 cm^{-1}) [39]. The second is that the measured and computed integrated intensities also coincide, with differences well smaller than the experimental uncertainty (roughly estimated to 20 % and 30 % for $^{12}CO_2$ and $^{13}CO_2$, respectively). The integrated band intensities for the two isotopologues are close, as could be expected from the fact that the CO_2 dipole matrix elements are practically identical [37,38]. Finally, the experimental and predicted HWHM are again consistent, both showing a negligible isotope effect, as could be expected from the strong similarity between $^{12}CO_2$ and $^{13}CO_2$.

	$\nu_3(^{12}CO_2)+\nu_1(H_2O)$		$\nu_3(^{13}CO_2)+\nu_1(H_2O)$	
	Exp	CMDS	Exp	CMDS
Center (cm^{-1})	5998.4	5999.7	5930.2	5932
Integrated binary coefficient (10^{-3} cm^{-2}amagat^{-2})	2.6	2.08	2.1	2.06
HWHM (cm^{-1})	33.0	31	28.2	31

Table 1: *Band centers, integrated intensities and half widths at half maximum (HWHM) of the $\nu_3(CO_2)+\nu_1(H_2O)$ CIA bands measured and CMDS-calculated for natural $^{12}CO_2$ and in $^{13}CO_2$.*

A comparison between the measured and computed H_2O-$^{12}CO_2$ density-normalized absorption coefficients over the spectral range of the 1.6 μm window is displayed in **Fig. 4.** The calculated spectrum was obtained by adding the CIA predicted in the present study to the contributions of the far wings of the H_2O-broadened transitions of CO_2 and of the CO_2-broadened lines of H_2O. The associated values of the binary coefficients, $B_{CO_2-H_2O}$ and $B_{H_2O-CO_2}$, were calculated with the χ-factor approaches developed in Refs. [8] and [9] respectively. As can be seen, the agreement is quite satisfactory which validates the prediction of all three contributions. However there is a noticeable discrepancy between measured and computed values on the low frequency side of the CIA peak which may be explained by the neglecting of the contribution of the anisotropic polarizability $\Delta\alpha$ of H_2O in the CMDS computation of the collision-induced dipole. Indeed, first note that, since $\langle v = 0|\Delta\alpha(\mathrm{H_2O})|v_1 = 1\rangle = 0.54$ a. u. (obtained from the value of α_0^2 provided in Ref. [36] and $\Delta\alpha = \sqrt{3/2}\,\alpha_0^2$) which is smaller than $\langle v = 0|\alpha_{iso}(\mathrm{H_2O})|v_1 = 1\rangle = 0.73$ a. u. by a factor of about $\sqrt{2}$, the integrated intensity due to this dipole induction mechanism should be about 2 times lower. In addition, the anisotropic polarizability selection rule allows not only Q but also O and S lines associated with *J* → *J*±2 transitions, the latter being spread over a broad spectral range of several 100 cm^{-1} on both sides of the central vibrational frequency. In summary, this contribution, which is weaker and spectrally

much broader than that of the isotropic polarizability, may explain the above mentioned missing "background".

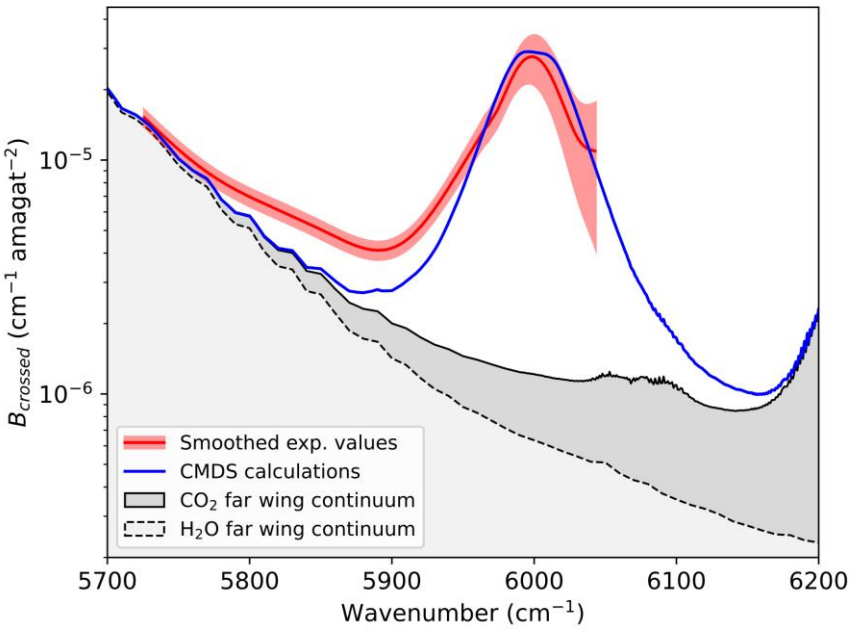

Fig 4: *Crossed binary coefficients in the region of the $\nu_3(^{12}CO_2)+\nu_1(H_2O)$ CIA band. The CIA predicted by CMDS calculations (blue) is added to the sum of the H_2O (light grey) and CO_2 (grey) far wing continua. Also shown are the smoothed experimental values from Ref. [10] (red, with a 1σ error band).*

It is worth mentioning that the $\nu_3(CO_2)+\nu_1(H_2O)$ CIA band presently measured in the gas phase at sub-atmospheric pressure was pointed out nearly three decades ago in liquid CO_2+H_2O mixtures, thus at considerably higher molecular densities [40]. Low resolution spectra were recorded with grating spectrographs allowing for an estimation of the integrated absorption cross-section. A value of 8×10^{-4} cm^{-2}amagat^{-2} was estimated in the liquid phase, about three times smaller than our gas phase value (2.6×10^{-3} cm^{-2}amagat^{-2}). Note that a similar tendency between liquid and gas phase CIA intensities (normalized to squared density) was reported for the far-infrared CIA of pure CO_2 [41].

In general, free collisions are believed to bring most of the contribution to CIA bands and H_2O-CO_2 bound complexes, which are disregarded in the CMDS, are not expected to contribute significantly to the observed absorption feature. The agreement between the measured and CMDS integrated band intensities seems to confirm this expectation. The H_2O-CO_2 bound complex which has been observed in matrices (e.g. [42]) and in expansion jets (e.g. [43,44]) has a planar T-shaped structure with hydrogens pointing away from CO_2. The dissociation energy D_0 was estimated to be about 730 cm^{-1} [45,46]. It is worth mentioning the results of anharmonic vibrational calculations of the spectrum of this Van der Waals complex [47], based on *ab initio* force field and electro-optical parameters. As expected, most of the predicted vibrational bands of the H_2O-CO_2 complex fall in coincidence with those of pure H_2O or CO_2 but, interestingly, Pavlyuchko et al. concluded their article by noting that

"…the combination transition $\nu_{OH}^{S} + \nu_{CO}^{as}$ [*e.g.* $\nu_3(CO_2)+\nu_1(H_2O)$] in the vicinity of $\sim$ 6000 cm^{-1}, falls occasionally in the regions of relative transparency of both isolated monomers and can therefore be discriminated from the monomer absorption" [47]. Although our observation cannot be interpreted as an absorption band of the H_2O-CO_2 bound complex, the above statement about the detection of simultaneous transitions applies to the CIA in (H_2O+CO_2) gas mixtures.

5. Conclusion

The present study, thanks to measurements and classical molecular dynamics calculations made for both $^{12}CO_2$-H_2O and $^{13}CO_2$-H_2O mixtures, has confirmed that the band observed around 6000 cm^{-1} in Ref. [10] is indeed due to the dipole induced in interacting (CO_2, H_2O) pairs through the $\nu_3(CO_2)+\nu_1(H_2O)$ simultaneous transitions, involving an absorption (CO_2) and a Raman (H_2O) process. It is worth emphasizing that this is the first demonstration of a purely collision-induced absorption contribution to the binary continuum in CO_2 + H_2O gas mixtures, which was so far entirely attributed to the far line wings of the dipole transitions of CO_2 broadened by H_2O and of H_2O broadened by CO_2.

Note that other simultaneous transitions in H_2O+CO_2 gas mixtures exist which may be detectable, since centered in some relatively transparent regions of the H_2O+CO_2 spectrum, and thus deserve investigation. The first [$\nu_3(CO_2)+\nu_3(H_2O)$] is similar to the one studied in this paper, but in which a H_2O ν_3 Raman vibrational change is involved, which would lead to a CIA centered around 6105 cm^{-1}. This CIA is expected to be small and broad, since $\langle v=0|\alpha_{iso}(\mathrm{H_2O})|v_3=1\rangle = 0$ [36] and thus only the $\langle v=0|\Delta\alpha(\mathrm{H_2O})|v_3=1\rangle$ matrix element contributes. Another contribution comes from the $\nu_2(CO_2)+\nu_1(H_2O)$ transition, involving, among others, the contributions of the products $\langle v=0|\Delta\alpha(\mathrm{H_2O})\text{ and }\alpha_{iso}(\mathrm{H_2O})|v_1=1\rangle\langle v=0|\mu(\mathrm{CO_2})|v_2=1\rangle$, which for $^{12}CO_2$ should peak near 4334 cm^{-1}. The associated CIA band is expected to be less intense than the one investigated in this study due to the smaller central wavenumber and weaker CO_2 dipole matrix element ($\langle v=0|\mu(\mathrm{CO_2})|v_2=1\rangle = 0.071$ a.u. [33,34]). For completeness, note that two other simultaneous transitions should appear around 2900 cm^{-1}, $\nu_1(CO_2)+\nu_2(H_2O)$ and $2\nu_2(CO_2)+\nu_2(H_2O)$, associated with the polarization of CO_2 by the dipole of H_2O, through the product $\langle v=0|\Delta\alpha(\mathrm{CO_2})\text{ and }\alpha_{iso}(\mathrm{CO_2})|v_1=1\text{ or }v_2=2\rangle\langle v=0|\mu(\mathrm{H_2O})|v_2=1\rangle$.

Acknowledgements

This work was performed in the frame of the ANR project COMPLEAT (ANR-19-CE31-0010-01). H. Tran and M. Turbet (LMD) are thanked for providing the $B_{CO_2-H_2O}$ and $B_{H_2O-CO_2}$ binary coefficients calculated with the χ-factor approach. AC is grateful to Andrey Vigasin for useful exchanges. WF and J-MH thank Prof. Christian Boulet for very helpful discussions.

References

[1] Hartmann J-M, Tran H, Armante R, Boulet C, Campargue A, Forget F, Gianfrani L, Gordon I, Guerlet S, Gustafsson M, Hodges JT, Kassi S, Lisak D, Thibault F, Toon GC. Recent advances in collisional effect on spectra of molecular gases and their practical consequences. J Quant Spectrosc Radiat Transf 2018;213:178–227. doi:10.1016/j.jqsrt.2018.03.016.

[2] Hartmann J-M, Boulet C, Robert D. Collisional effects on molecular spectra: laboratory experiments and models, consequences for applications. Elsevier; 2021. Second Edition Amsterdam.

[3] Hartmann J-M, Boulet C, Tran DD, Tran H, Baranov Y. Effect of humidity on the absorption continua of CO_2 and N_2 near 4 μm: Calculations, comparisons with measurements, and consequences for atmospheric spectra. J Chem Phys 2018;148:054304. doi:10.1063/1.5019994.

[4] Hartmann J-M, Armante R, Toon GC, Scott N, Tran H, Crevoisier C, Chédin A, Capelle V. Indirect influence of humidity on atmospheric spectra near 4 μm. Geophys Res Lett 2018;45;12593–12601. doi:10.1029/2018GL079582.

[5] Ma Q, Tipping RH. A far wing line shape theory and its application to the foreign-broadened water continuum absorption. III. J Chem Phys 1992;97:818–828. doi:10.1063/1.463184.

[6] Pollack JB, Dalton JB, Grinspoon D, Wattson RB, Freedman R, Crisp D, Allen DA, Bézard B, DeBergh C, Giver LP, Ma Q, Tipping RH. Near-Infrared Light from Venus' Nightside: A Spectroscopic Analysis. Icarus 1993;103:1–42. doi:10.1006/icar.1993.1055.

[7] Baranov YI. On the significant enhancement of the continuum-collision induced absorption in H_2O+CO_2 mixtures. J Quant Spectrosc Radiat Transf 2016;175:100–6. doi:10.1016/j.jqsrt.2016.02.017.

[8] Tran H, Turbet M, Chelin P, Landsheere X. Measurements and modeling of absorption by CO_2+H_2O mixtures in the spectral region beyond the CO_2 ν_3-band head. Icarus 2018;306:116–121. doi:10.1016/j.icarus.2018.02.009.

[9] Tran H, Turbet M, Hanoufa S, Landsheere X, Chelin P, Ma Q, Hartmann J-M. The CO_2–broadened H_2O continuum in the 100–1500 cm^{-1} region: Measurements, predictions and empirical model. J Quant Spectrosc Radiat Transf 2019;230:75–80. doi:10.1016/j.jqsrt.2019.03.016.

[10] Fleurbaey H, Campargue A, Carreira Mendès da Silva Y, Grilli R, Kassi S, Mondelain D. Characterization of the foreign water vapor continuum in CO_2 within the infrared transparency windows. J Quant Spectrosc Radiat Transf submitted.

[11] Mondelain D, Campargue A, Čermák P, Gamache RR, Kassi S, Tashkun SA, Tran H. The CO_2 absorption continuum by high pressure CRDS in the 1.74 μm window. J Quant Spectrosc Radiat Transfer 2017;203:530–537. doi:10.1016/j.jqsrt.2017.02.019.

[12] Brodbeck C, Bouanich J-P, Figuiere P, Szwarc H. Simultaneous infrared transitions in N_2 + SF_6 mixtures. J Chem Phys 1981;74:77–80. doi:10.1063/1.440796.

[13] Bouanich J-P, Brodbeck C. Collision-induced simultaneous transitions in H_2+CF_4 and H_2+SF_6 mixtures. J Quant Spectrosc Radiat Transf 1977;17:777–82. doi:10.1016/0022-4073(77)90041-3.

[14] Abu-Kharma M. Analysis of the collision-induced absorption spectra of H_2 in H_2–N_2 in the range 5600–9500 cm^{-1}. J Phys B: At Mol Opt Phys 2007;40:2345–50. doi:10.1088/0953-4075/40/12/010.

[15] Stamp S, Prasad RDG, Gillard PG, Paddi Reddy S. Analysis of the collision-induced absorption spectra of double vibrational transitions in H_2–N_2", AIP Conference Proceedings 1999;467:453–456. doi:10.1063/1.58384.

[16] Tonkov MV, Filippov NN, Bertsev VV, Bouanich JP, Nguyen Van Thanh, Brodbeck C, et al. Measurements and empirical modelling of pure CO_2 absorption in the 2.3 μm region at room temperature: far wings, allowed and collision-induced bands. Appl Opt 1996;35:4863–70. doi:10.1364/AO.35.004863.

[17] Fahrenfort J, Ketelaar JAA. Simultaneous Vibrational Transitions in the Infrared Absorption Spectra of Compressed Gases. J Chem Phys 1954;22:1631. doi:10.1063/1.1740502.

[18] Keteelar JAA. Infra-red spectra of compressed gases. Spectrochim Acta 1959;14:237–248. doi:10.1016/0371-1951(59)80231-9.
[19] Brodbeck C, Bouanich J-P, Penner AR, Meinander N, Tabisz GC. Band-shape analysis of an infrared double transition in CO_2 + N_2 gas mixtures. Can J Phys 1987;65:1073–1076. doi:10.1139/p87-177.
[20] Maté B, Fraser GT, Lafferty WJ. Intensity of the simultaneous vibrational absorption CO_2 (v_3=1) + N_2 (v=1) ← CO_2 (v_3=0) + N_2 (v=0) at 4680 cm^{-1}. J Mol Spectrosc 2000;201:175–177. doi:10.1006/jmsp.2000.8074.
[21] Brown A, Tipping RH, Maté B. Theoretical Study of the Collision-Induced Double Transition CO_2 (v_3=1) + N_2 (v_1=1) ← CO_2 (v_3=0) + N_2 (v_1=0) at 296 K. J Mol Spectrosc 2000;204(1):153–158. doi:10.1006/jmsp.2000.8214.
[22] Kassi S, Campargue A, Mondelain D, Tran H. High pressure Cavity Ring Down Spectroscopy: Application to the absorption continuum of CO_2 near 1.7 µm. J Quant Spectrosc Radiat Transf 2015;167:97–104. doi:10.1016/j.jqsrt.2015.08.014.
[23] Campargue A, Kassi S, Mondelain D, Vasilchenko S, Romanini D. Accurate laboratory determination of the near infrared water vapor self-continuum: A test of the MT_CKD model. J Geophys Res Atmos 2016;121:13180–13203. doi:10.1002/2016JD025531.
[24] Lechevallier L, Vasilchenko S, Grilli R, Mondelain D, Romanini D, Campargue A. The water vapour self-continuum absorption in the infrared atmospheric windows: new laser measurements near 3.3 and 2.0 µm. Atmos Meas Tech 2018;11:2159–2171. doi:10.5194/amt-11-2159-2018.
[25] Richard L, Vasilchenko S, Mondelain D, Ventrillard I, Romanini D, Campargue A. Water vapor self-continuum absorption measurements in the 4.0 and 2.1 µm transparency windows. J Quant Spectrosc Radiat Transf 2017;201:171–179. doi:10.1016/j.jqsrt.2017.06.037.
[26] Ventrillard I, Romanini D, Mondelain D, Campargue A. Accurate measurements and temperature dependence of the water vapor self-continuum absorption in the 2.1 µm atmospheric window. J Chem Phys 2015;143:134304. doi:10.1063/1.4931811.
[27] Vasilchenko S, Campargue A, Kassi S, Mondelain D. The water vapour self- and foreign-continua in the 1.6 µm and 2.3 µm windows by CRDS at room temperature. J Quant Spectrosc Radiat Transf 2019;227:230–238. doi:10.1016/j.jqsrt.2019.02.016.
[28] Fleurbaey H, Grilli R, Mondelain D, Campargue A. Measurements of the water vapor continuum absorption by OFCEAS at 3.50 µm and 2.32 µm. J Quant Spectrosc Radiat Transf 2022;278:108004. doi:10.1016/j.jqsrt.2021.108004.
[29] Fleurbaey H, Reed ZD, Adkins EM, Long DA, Hodges JT. High accuracy spectroscopic parameters of the 1.27 µm band of O_2 measured with comb-referenced, cavity ring-down spectroscopy. J Quant Spectrosc Radiat Transf 2021;270:107684. doi:10.1016/j.jqsrt.2021.107684.
[30] Mondelain D, Kassi S, Campargue A. Accurate laboratory measurement of the O_2 collision-induced absorption band near 1.27 µm. J Geophys Res: Atmospheres 2019;124:414–423. doi:10.1029/2018JD029317.
[31] Kassi S, Guessoum S, Abanto JCA, Tran H, Campargue A, Mondelain D. Temperature dependence of the collision-induced absorption band of O_2 near 1.27 µm. J Geophys Res: Atmospheres 2021;126:e2021JD034860. doi:10.1029/2021JD034860.
[32] Gordon IE, Rothman LS, Hill C, Kochanov RV, Tan Y, Bernath PF, Birk M, Boudon V, Campargue A, et al. The HITRAN2016 Molecular Spectroscopic Database. J Quant Spectrosc Radiat Transf 2017;203:3–69. doi:10.1016/j.jqsrt.2017.06.038.
[33] Kolomiĭtsova TD, Lyaptsev AV, Shchepkin DN. Determination of parameters of the dipole moment of the CO_2 molecule. Opt Spectrosc 2000;88:648–60. doi:10.1134/1.626856.
[34] Liang Z, Tsai HL. Determination of vibrational energy levels and transition dipole moments of CO_2 molecules by density functional theory. J Mol Spectrosc 2008;252:108–14. doi:10.1016/j.jms.2008.07.008.
[35] Frommhold L. Collision Induced Absorption in Gases. Cambridge Monographs on Atomic, Molecular, and Chemical Physics. Cambridge University Press, Cambridge, (2006).
[36] Avila G, Fernández JM, Tejeda G, Montero S. The Raman spectra and cross-sections of H_2O, D_2O, and HDO in the OH/OD stretching regions. J Mol Spectrosc 2004;228:38-65. doi:10.1016/j.jms.2004.06.012.
[37] Johns JWC. Absolute intensities in CO_2: The 4.3- and 2.7-µm regions revisited. J Mol Spectrosc 1989;134:433-9. doi:10.1016/0022-2852(89)90328-7.

[38] Gordon IE, Rothman LS, Hargreaves RJ, Hashemi R, Karlovets EV, Skinner FM, Conway EK, Hill C, et al. The HITRAN2020 Molecular Spectroscopic Database. J Quant Spectrosc Radiat Transf 2022;277:107949. doi:10.1016/j.jqsrt.2021.107949.

[39] Rothman LS, Hawkins RL, Wattson RB, Gamache RR. Energy levels, intensities, and linewidths of atmospheric carbon dioxide bands. J Quant Spectrosc Radiat Transf 1992;48:537–66. doi:10.1016/0022-4073(92)90119-O.

[40] Vigasin AA, Adiks TG, Tarakanova EG, Yukhnevich GV. Simultaneous infrared absorption in a mixture of CO_2 and H_2O: The role of hydrogen-bonded aggregates. J Quant Spectrosc Radiat Transf 1994;52:295-301. doi:10.1016/0022-4073(94)90159-7.

[41] Ho W, Birnbaum G, Rosenberg A. Far-infrared collision-induced absorption in CO_2. I. Temperature dependence. J Chem Phys 1971;55:1028. doi:10.1063/1.1676181

[42] Schriver A, Schriver-Mazzuoli L, Chaquin P, Dumont E. FTIR and ab Initio Study of the 1/1 Complex between Water and Carbon Dioxide in Solid Nitrogen. J Phys Chem A 2006;110:51–56. doi:10.1021/jp0581328.

[43] Zhu Y, Li S, Sun P, Duan C. Infrared diode laser spectroscopy of H_2O–CO_2 and D_2O–CO_2 complexes in the v_2 bend region of water. J Mol Spectrosc 2013;283:7–9. doi:10.1016/j.jms.2012.12.002.

[44] Bogomolov AS, Roucou A, Bejjani R, Herman M, Moazzen-Ahmadi N, Lauzin C. The rotationally resolved symmetric 2OH excitation in H_2O-CO_2 observed using pulsed supersonic expansion and CW-CRDS. Chem Phys Letters 2021;774:138606. doi:10.1016/j.cplett.2021.138606.

[45] Makarewicz J. Intermolecular potential energy surface of the water-carbon dioxide complex. J Chem Phys 2010;132:234305. doi:10.1063/1.3439693.

[46] Andersen J, Heimdal J, Mahler DW, Nelander B, Wugt Larsen R, et al. Communication: THz absorption spectrum of the CO_2–H_2O complex: Observation and assignment of intermolecular van der Waals vibrations. J Chem Phys 2014;140:091103. doi:10.1063/1.4867901.

[47] Pavlyuchko AI, Orlinson BS, Vigasin AA. Variational Solution of Anharmonic Vibrational Problems for Polyatomics and Molecular Pairs. In: Camy-Peyret C, Vigasin AA (eds) Weakly Interacting Molecular Pairs: Unconventional Absorbers of Radiation in the Atmosphere. NATO Science Series (Series IV: Earth and Environmental Sciences), vol 27. Springer, Dordrecht. 2003, pp. 73–82. doi:10.1007/978-94-010-0025-3_5.